Trace Gas Emissions from Biomass Burning inferred from Aerosol Optical Depth

Clare Paton-Walsh
University of Wollongong, clarem@uow.edu.au

N. B. Jones
University of Wollongong, njones@uow.edu.au

Stephen R. Wilson
University of Wollongong, swilson@uow.edu.au

A. Meier
University of Wollongong

N. Deutscher
University of Wollongong

See next page for additional authors

Recommended Citation

Trace Gas Emissions from Biomass Burning inferred from Aerosol Optical Depth

Abstract

We have observed strong correlations between simultaneous and co-located measurements of aerosol optical depth and column amounts of carbon monoxide, hydrogen cyanide, formaldehyde and ammonia in bushfire smoke plumes over SE Australia during the Austral summers of 2001/2002 and 2002/2003. We show how satellite-derived aerosol optical depth maps may be used in conjunction with these correlations to determine the total amounts of these gases present in a fire-affected region. This provides the basis of a method for estimating total emissions of trace gases from biomass burning episodes using visible radiances measured by satellite.

Keywords

GeoQUEST

Disciplines

Life Sciences | Physical Sciences and Mathematics | Social and Behavioral Sciences

Publication Details

Authors

Clare Paton-Walsh, N. B. Jones, Stephen R. Wilson, A. Meier, N. Deutscher, D. W. Griffith, R. Mitchell, and S. Campbell

Trace Gas Emissions from Biomass Burning inferred from Aerosol Optical Depth

Clare Paton-Walsh, Nicholas Jones, Stephen Wilson, Arndt Meier, Nicholas Deutscher and David Griffith
Department of Chemistry, University of Wollongong, Australia.

Ross Mitchell and Susan Campbell
CSIRO Atmospheric Research, Earth Observation Centre, Canberra, Australia.

Abstract

We have observed strong correlations between simultaneous and co-located measurements of aerosol optical depth and column amounts of carbon monoxide, hydrogen cyanide, formaldehyde and ammonia in bushfire smoke plumes over SE Australia during the Austral summers of 2001/2002 and 2002/2003. We show how satellite-derived aerosol optical depth maps may be used in conjunction with these correlations to determine the total amounts of these gases present in a fire-affected region. This provides the basis of a method for estimating total emissions of trace gases from biomass burning episodes using visible radiances measured by satellites.

Introduction

Biomass burning releases large amounts of trace gases and particulates into the atmosphere, significantly affecting global atmospheric chemistry, degrading air quality, and impacting on radiative transfer in the atmosphere [*Crutzen and Andreae*, 1990]. A change in the incidence of fires is expected due to future variations in global climate, providing a potential feedback mechanism for climate change. Despite the significance of these emissions, quantifying the amount of each gas emitted in forest fires remains a difficult process and a new technique for estimating emissions could be an extremely useful complementary tool.

Measurements and Analysis

During the 2001/2002 and 2002/2003 austral summers, we recorded more than seventeen hundred infrared solar atmospheric absorption spectra at Wollongong NSW, Australia (34.5°S, 150°E) through smoke plumes originating from many different bush-fires. Simultaneous and co-located direct solar spectral irradiance measurements spanning the visible wavelengths were also made, so that the optical depth of the atmosphere during the time of the infrared measurements could be determined. The infrared solar atmospheric absorption spectra were recorded using a Bomem DA8 high-resolution Fourier transform infrared spectrometer coupled to a solar tracker that transmits the direct solar beam to the entrance aperture of the spectrometer. The tracker has both active and passive tracking systems and is able to follow the sun through smoke plumes that are opaque to the human eye. Spectra were recorded in a number of regions of the infrared from 700 cm^{-1} to 4500 cm^{-1} using Mercury Cadmium Telluride and Indium Antimonide detectors, and a series of eight different optical band pass filters [*Griffith et al.*, 1998]. The number of molecules per square centimetre above the measurement site (the vertical column amounts) of carbon monoxide (CO), ammonia (NH$_3$), formaldehyde (H$_2$CO) and hydrogen cyanide (HCN) were derived from individual spectra from the appropriate filter regions, using the iterative fitting algorithm known as SFIT2 [*Rinsland et al.*, 1998], In this study the concentration profiles used for the initial simulation were typical of "clean air" and the analysis was weighted to allow very large variability in the boundary layer and lower troposphere to achieve a good fit.

Spectral irradiance was measured using an Ocean Optics OD2000 grating spectrometer with a 2048 pixel CCD detector array spanning the visible wavelengths. The measurements were calibrated using the Langley technique to derive the top of the atmosphere signal from data

collected on clear days before, during and after the smoke measurements [*Wilson and Forgan*, 2002]. Individual estimates of aerosol optical depth (AOD) at 500 nm were derived from each measurement of irradiance through subtraction of the Rayleigh scattering component, and the mean value calculated for the period of time taken to record each of the infrared spectra. Although our measurements span the visible spectrum, maximum signal intensity and minimum interference by molecular absorbance is obtained at 500nm. . AOD values greater than 0.1 can result from cloud cover as well as smoke, however since cloud strongly attenuates the mid-infrared signal, the quality of the infrared spectra confirms the presence of smoke.

This dataset of vertical column amounts of gases with coincident AOD values encompasses measurements made on thirty-four separate days, through smoke plumes originating from bushfires only a few kilometres away to distant bushfires hundreds of kilometres away. These measurements constitute a varied sample, which we believe is representative of typical Australian temperate forest fires.

Correlations of trace gas amounts with AOD

Figure 1 shows vertical column amounts of CO plotted against the simultaneous, co-located measurements of AOD. The error-bars shown in column amounts of CO represent the expected one-sigma precision of the measurements, which illustrates the scatter expected from the measurement repeatability. The error-bars shown in the AOD measurements combine an uncertainty from the calibration with the one-sigma standard deviation of the measurements. The latter includes both the real variation in AOD (due to varying amounts of smoke) and variability of the CCD measurement. The data have been colour coded to distinguish different time periods. The correlation between column CO and AOD shown in figure 1 is consistent for more than

three hundred independent spectra from many varied forest fire episodes over all the different time periods, with the exception of the spectra recorded on January 1st 2002.

Figures 2a, 2b and 2c show vertical column amounts of HCN, H$_2$CO and NH$_3$ plotted against simultaneous measurements of aerosol optical depth, colour coded as in figure 1. On January 1st 2002 there was thick ground-level smoke in the morning. Two spectra were recorded in the spectral region used to derive NH$_3$, followed by two more spectra in a region used to derive CO before the arrival of a distinctive smoke plume was noted. After the arrival of this plume all four graphs show the same exceptional behaviour, with very large amounts of the trace gases seen around noon and much larger trace gas-to-AOD ratios. The thick smoke plume sampled on January 1st 2002 could be from a single nearby fire, in which the fuels burnt differed significantly from the normal mixture sampled on the other 33 days. Whatever the reason, the data is clearly exceptional with relatively low AOD values while other molecule-molecule correlations remain consistent with other data.

Figures 2a and 2b show that HCN and H$_2$CO are also highly correlated with AOD. The scatter is larger than for CO-to-AOD, however the lower precision in the column measurements of these gases (note the larger error bars) make it difficult to distinguish the higher natural variability in the emissions of these compounds that has been seen in previous studies[*Yokelson et al.*, 2003]. In contrast, the scatter apparent in figure 2c is significantly larger than the measurement precision, but the colour coding reveals a much stronger correlation of NH$_3$ with AOD during individual time periods, especially December 2002 – January 2003 (R^2 = 0.93). NH$_3$ is more reactive and shorter-lived than the other species and the large overall scatter seen in figure 2c probably results as much from differences in the local humidity levels, aerosol

scavenging, and the age of the smoke as from differences in the relative emission rates of NH_3 from the fires.

Emission ratios of biomass burning indicators

Trace gas concentrations within smoke plumes can vary rapidly with time, so the concentration levels are usually converted to relative emission ratios by dividing by coincident measurements of CO or CO_2 [*Hurst et al.*, 1994]. Our chosen reference gas is CO, because the excess levels of CO_2 present in smoke are difficult to measure with sufficient accuracy against its large background amount. In this study we have no coincident measurements of CO with the other trace gases because the column amounts are derived from spectra recorded at different times using different optical filters. Instead we have calculated emission ratios for HCN, H_2CO and NH_3 with respect to CO, using AOD as a de-facto measurement of the CO column via the correlation shown in Figure 1.

We calculated emission ratios by dividing the excess amount of the trace gas over background levels by the excess amount of CO over background levels. Mean column values from 1996 – 2000 were used as background levels: (1.6 ± 0.5 x10^{18} for CO; 4.3 ± 0.8 x10^{15} for HCN; 3.6 ± 0.3 x10^{15} for H_2CO and 2.1 ± 2.1 x10^{15} for NH_3). Previously published emission ratios show broad variations, but those calculated here for HCN (0.0048 ± 0.0041) and H_2CO (0.019 ± 0.008) are close to the literature average for forest fuels [*Goode et al.*, 2000; *Yokelson et al.*, 2003; *Yokelson et al.*, 1999].The measurements described here have the advantage of being vertically integrated through smoke plumes from a natural range of fuels and fire conditions. The NH_3 emission ratio that we calculate (0.0073 ± 0.0043) is lower than previous measurements in forest fires but we are probably measuring older smoke where the NH_3 has

been scavenged by moisture and aerosol in the air [*Goode et al.*, 2000]. Separate emission ratios calculated for January 1st 2002 were comparable with those measured for all other days, suggesting that a lower emission of particles is responsible for the anomalous data.

A Potential Method for Estimating biomass burning emissions

The difficulty of estimating the total mass of fuel burned is a major limitation to traditional methods of estimating emissions from biomass burning, especially on a global scale. The trace gas-to-AOD correlations presented here suggest an alternative approach based on satellite-derived AOD data. In previous studies, good agreement has been found between ground-based sun photometer measurements of AOD (as used in this study) and satellite derived AOD measurements [*Schmid et al.*, 2003]. Thus the gas-to-AOD correlations shown in figures 1 and 2 can be used to translate directly from the satellite-measured AOD into an estimated column amount of each trace gas present in a fire-affected region.

Figure 3 shows enhanced values of AOD on January 26th 2003 generated by the bushfires that burned for several weeks beginning January 12th 2003 in the alpine areas of South-eastern Australia. The data were obtained from the Moderate Resolution Imaging Spectroradiometer (MODIS) instruments on board the NASA Earth Observing System satellites Terra (daily pass, 11:05 local time) and Aqua (daily pass, 15:20 local time) [*Chu et al.*, 2002; *Remer et al.*, 2002]. The white pixels indicate areas where the retrieved AOD was below the detection threshold of 0.05 or has been rejected by the retrieval algorithm, for example through contamination by cloud or sun-glint.

The AOD values at 500 nm measured by the MODIS instruments above Wollongong on January 26th 2003 were 1.1 ± 0.1 and 1.0 ± 0.1 respectively, compared to our ground-based sun-photometer measurements of AOD of 1.3 ± 0.3. The satellite measurements are integrated over a

10 km square area at two distinct times, whereas the sun-photometer readings sample less than 1 m square but are averaged over the day. Therefore the values are only expected to be broadly comparable

Included in figure 3 are the column amounts of CO, HCN or H_2CO derived by applying the relationships given in figures 1 and 2. If the vertical distribution of the smoke is also known, this mapping of column amounts of biomass burning products could be used to infer ground level concentrations of trace gases. Although column measurements alone are not good indicators for the ground-level concentration, when coupled with meteorological transport models these images might provide useful estimates of average exposure levels where no ground based measurements exist [*Chu et al.*, 2003; Wang and Christopher, 2003].].

Moreover the mapping of column amounts illustrated in figure 3 provides the basis of a method for estimating total emissions of trace gases from biomass burning episodes. The total amount of each trace gas present at any one time can be found by integrating over the total area of the plume, but integration over time is also needed to get a total emissions estimate. Satellite radiance measurements can confirm the presence of fires [*Dozier*, 1980], and so the duration of a fire episode may be estimated with a time resolution defined by the time between each satellite pass over the area of interest. Each time the satellite passes overhead it can make a new measurement of the AOD, and hence the total amount of trace gases present in a defined "active" region. The total flux out of (or into) the active region during the time between satellite passes can be estimated by combining the average horizontal components of the tropospheric wind velocity with the average column amount of trace gas present at the boundaries of the active region. Thus the integrated total flux of a trace gas out of the active region during the lifetime of

the fire episode may be added to the total amount of the trace gas present in the region at the end of the episode, to give the total amount of gas emitted.

The major uncertainties in this methodology are probably uncertainties in tropospheric wind velocities and uncertainties in the trace-gas-to-AOD ratios. These ratios have only been measured for Australian forest fires and further measurements of this type are required to extend this method to other geographical regions or fires types. Another limitation is that the technique cannot be used if cloud cover inhibits the satellite AOD measurements. Also the smoke must dissipate out of the defined active region (where the fires are burning) before the trace-gas-to-AOD ratios change significantly as a result of the different atmospheric lifetimes of the various components: (hours for NH_3 and H_2CO; days for the particulate matter that causes elevated AOD; 1-2 months for CO and approximately 3 months for HCN) [*Li et al.*, 2000; *Mauzerall et al.*, 1998].

Despite these limitations, we believe that the measurements described here reveal a powerful new method for estimating emissions from biomass burning. The dominant uncertainties in the proposed methodology are different from those in traditional estimates, making this an ideal complementary technique.

References and Notes

Chu, D.A., et. al., Validation of MODIS aerosol optical depth retrieval over land, *Geophysical Research Letters*, *29* (12), 8007, 2002.

Chu, D.A., et. al., Global monitoring of air pollution over land from the Earth Observing System-Terra Moderate Resolution Imaging Spectroradiometer (MODIS), *Journal of Geophysical Research*, *108*, 4661, 2003.

Crutzen, P.J., and M.O. Andreae, Biomass burning in the tropics: Impact on atmospheric chemistry and biogeochemical cycles, *Science*, *250* (1669), 1990.

Dozier, J., Satellite identification of surface radiant temperature fields of subpixel resolution, N.O.A.A., Washington D.C., 1980.

Goode, J.G., et. al., Measurements of excess O3, CO2, CO, CH4, C2H4, C2H2, HCN, NO, NH3, HCOOH, CH3COOH, HCHO, and CH3OH in 1997 Alaskan biomass burning plumes by airborne Fourier transform infrared spectroscopy (AFTIR), *Journal of Geophysical Research*, *105*, 22147-22166, 2000.

Griffith, D.W.T., et. al., Interhemispheric ratio and annual cycle of carbonyl sulfide (OCS) total column from ground-based solar FTIR spectra, *Journal of Geophysical Research*, *103* (D7), 8447-8454, 1998.

Hurst, D.F., et. al., Trace gas emissions from biomass burning in tropical Australian savannas, *Journal of Geophysical Research*, *99* (D8), 16,441 - 16,456, 1994.

Li, Q.B., et. al., Atmospheric hydrogen cyanide (HCN): Biomass burning source, ocean sink?, *Geophysical Research Letters*, *27*, 357-360, 2000.

Mauzerall, D.L., et. al., Photochemistry in biomass burning plumes and implications for tropospheric ozone over the tropical South Atlantic, *Journal of Geophysical Research*, *103*, 8401-8423, 1998.

Remer, L.A., et. al., Validation of MODIS aerosol retrieval over ocean, *Geophysical Research Letters*, *29* (12), 8008, 2002.

Rinsland, C.P., et. al., Northern and Southern Hemisphere Ground-Based Infrared Spectroscopic Measurements of Tropospheric Carbon Monoxide and Ethane, *Journal of Geophysical Research*, *103*, 28,197-28,218, 1998.

Schmid, B., et. al., Coordinated airborne, spaceborne, and ground-based measurements of massive thick aerosol layers during the dry season in southern Africa,, *Journal of Geophysical Research-Atmospheres*, *108* (D13), 2003.

Wang, J., and S.A. Christopher, Intercomparison between satellite-derived aerosol optical thickness and PM2.5 mass: Implications for air quality studies, *Geophysical Research Letters*, *30* (21), 2095, 2003.

Wilson, S.R., and B.W. Forgan, Aerosol optical depth at Cape Grim, Tasmania, 1986 -1999, *Journal of Geophysical Research*, *107* (D8), 2002.

Yokelson, R.J. et. al., Trace gas measurements in nascent, aged, and cloud processed smoke from African savanna fires by airborne Fourier transform infrared spectroscopy (AFTIR), *Journal of Geophysical Research*, *108*, 8478, 2003.

Yokelson, R.J., et. al., Emissions of formaldehyde, acetic acid, methanol, and other trace gases from biomass fires in North Carolina measured by airborne Fourier transform infrared spectroscopy, *Journal of Geophysical Research*, *104* (D23), 30,109-30,125, 1999.

Figure Captions:

Figure 1: Vertical column amounts of carbon monoxide derived from 326 separate spectra plotted against coincident measurements of AOD. (Only 326 of > 1700 spectra were recorded using optical filters covering regions of the infra-red that contain CO absorption features.) The * symbol indicates the two spectra that were recorded just prior to the observation of a distinctive, thick smoke plume on January 1st 2002. The regression equation excludes data from January 1st 2002.

Figure 2: Panels a, b and c show vertical columns of hydrogen cyanide, formaldehyde and ammonia derived from 194, 188 and 184 spectra respectively, from the appropriate filter regions, plotted against coincident measurements of AOD. The * symbol in panel c indicates the two spectra taken on the MCT detector prior to the arrival of a distinctive, thick smoke plume on January 1st 2002. The regression equations exclude data from January 1st 2002.

Figure 3: Distribution of AOD at 500 nm over the Southeast coast of Australia on January 26th 2003 obtained from the MODIS aerosol product (MOD04), as observed from the Terra (left panel) and Aqua (right panel) platforms. The AOD scale has been converted to column amounts of CO, HCN or H_2CO by applying the relationships derived from figures 1and 2.
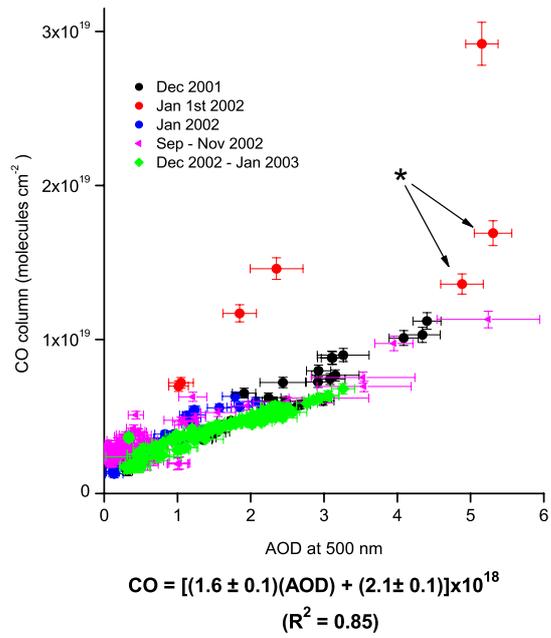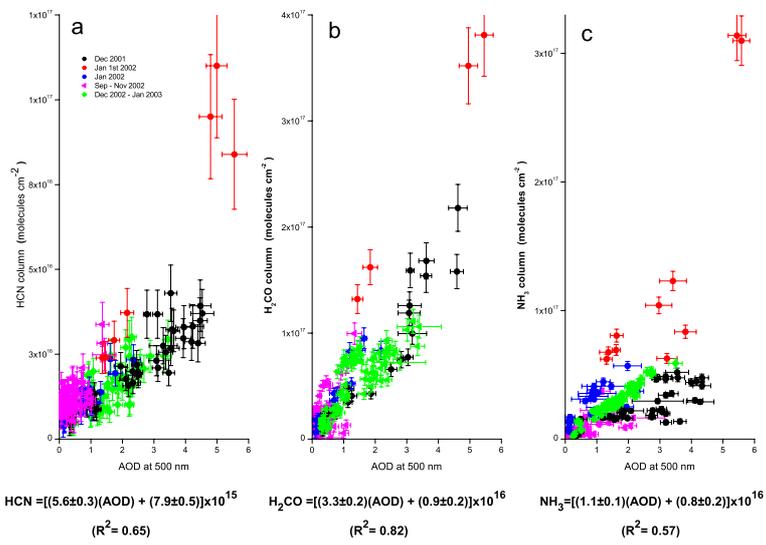
$$CO = [(1.6 \pm 0.1)(AOD) + (2.1 \pm 0.1)] \times 10^{18}$$

$$(R^2 = 0.85)$$

Figure 2:

HCN = [(5.6±0.3)(AOD) + (7.9±0.5)]x10^{15}

(R^2= 0.65)

H_2CO = [(3.3±0.2)(AOD) + (0.9±0.2)]x10^{16}

(R^2= 0.82)

NH_3=[(1.1±0.1)(AOD) + (0.8±0.2)]x10^{16}

(R^2= 0.57)

Figure 3: